JOURNAL OF MECHANICAL ENGINEERING AND SCIENCES (JMES)
ISSN: 2289-4659 e-ISSN: 2231-8380
VOL. 16, ISSUE 2, 8837 – 8847
DOI: https://doi.org/10.15282/jmes.16.2.2022.03.0699

ORIGINAL ARTICLE

Mathematical modelling of boundary layer flow over a permeable and time-dependent shrinking sheet – A stability analysis

J.G. Tan[1], Y.Y. Lok[1] and I. Pop[2]

[1] Mathematics Section, School of Distance Education, Universiti Sains Malaysia, 11800 USM, Penang, Malaysia.
Phone: +6046533931; Fax: +6046576000
[2] Department of Mathematics, Babeş-Bolyai University, 400084 Cluj-Napoca, Romania.

ABSTRACT – Micropolar fluid is one type of non-Newtonian fluid which consists of non-deformable spherical particles that suspended in viscous medium. In this paper, the problem of two-dimensional boundary layer flow over a permeable shrinking sheet with time dependent velocity in strong concentration micropolar fluid is studied theoretically. The mathematical model is governed by continuity, momentum and microrotation equations. Similarity variables are introduced so that, after performing the similarity transformation on the governing equations, the resulting system of nonlinear ordinary differential equations is then numerically solved using the program *bvp4c* in Matlab software. The effects of the micropolar material parameter, the unsteadiness parameter, the shrinking parameter and the mass suction parameter to the skin friction coefficient, velocity profiles and microrotation profiles are investigated. It is found that triple solutions exist for some values of the parameters that were considered. Based on the stability analysis that was performed, it showed that only two branches of solutions are categorized as stable, whereas one solution branch is unstable.

ARTICLE HISTORY
Received: 19th Oct. 2020
Revised: 11th Feb. 2022
Accepted: 09th Mar. 2022

KEYWORDS
Numerical solutions
Micropolar fluid
Suction
Shrinking sheet
Stability analysis

INTRODUCTION

The mathematical model of micropolar fluids has been introduced by Eringen [1] in 1966. This kind of non-Newtonian fluid belongs to a category of fluids that has microscopic effects due to micromotions and the local structure of the elements of fluids. Physically, micropolar fluids can be defined as fluids containing spherical particles which are randomly oriented and suspended in the viscous medium, however, the deformation of the suspended particles is negligible [1, 2]. The presence of spherical particles can affect the hydrodynamics and the flow's heat transfer characteristics. In this model, the microscopic effects of the fluid particles are considered in the transport equation; hence, a new vector field that describes the angular velocity of the particles'microrotation is introduced. Thus, compared to the viscous (Newtonian) fluid model, an extra equation is added to the micropolar fluid model, representing the balance law of angular momentum while an additional microrotation parameter is introduced in the momentum equation. Micropolar fluid has been widely applied in manufacturing processes, especially in the field of polymer industries, metallurgy, and exotic lubricants. Review on the theory of micropolar fluids as well as its applications can be read from Łukaszewicz [2], Eringen [3], Ariman et al. [4, 5].

It seems that Willson [6] was the first to apply the boundary layer's concept to the micropolar fluids. Then, Peddieson [7] studied the steady stagnation-point flow in the micropolar fluid by applying the boundary layer theory. Gorla [8] analyzed the mixed convection flow over a vertical plate in micropolar fluids. He showed that micropolar fluids help in reducing the drag and the heat transfer rate when compared to viscous fluids. The Blasius boundary layer flows over a flat plate in micropolar fluids has been numerically solved by Rees and Bassom [9] using the Keller-box method. They discovered that a two-layer structure is formed when the distance measured from the forward edge of the flat plate is increased.

During the later decades, research on flow and heat transfer characteristics induced by stretching/shrinking sheets in the Newtonian and non-Newtonian fluid has been the focus of many studies because of their applications in some of the manufacturing processes, such as polymer industry, glass production [10], etc. For the case of shrinking problem, the surface of the sheet is shrunk towards a particular point where the fluid velocity would move away due to the movement of the sheet. It seems that Miklavčič and Wang [11] were the first to obtain the exact solution of the Navier-Stokes equations that is induced by a shrinking sheet. They found that a sufficiently large mass suction is required so that the solution of the flow over shrinking sheet exists. It is worth mentioning that Goldstein [12] has shown that the shrinking sheet flow can be considered as a backward flow in which the physical phenomenon is different from the stretching sheet. The same finding was reported by Yacob and Ishak [13] who studied the steady two-dimensional boundary layer flow towards a shrinking sheet and found that a larger suction is required for the solution to existing in micropolar fluids compared to viscous fluids. Bhattacharrya et al. [14] carried out the study of the flow of micropolar fluids that passed a permeable shrinking sheet by imposing the thermal radiation effects. The numerical results of the problem of the micropolar fluids' flow over a permeable stretching or shrinking sheet through a porous medium have been studied by

*CORRESPONDING AUTHOR | Y. Y. Lok | ✉ lokyy@usm.my

Rosali et al. [15]. Then, Turkyilmazoglu [16] obtained the exact solution for the same problem considered by Rosali et al. [15]. Roşca and Pop [17] numerically solved the boundary layer flow of a micropolar fluid towards a shrinking sheet with suction and the second-order slip velocity using the function bvp4c in Matlab. All the above-mentioned papers showed that dual solutions exist for the problem of micropolar fluids flowing past a shrinking sheet with suction.

In many industrial applications, steady flow is preferable so that the manufacturing process can be easily controlled. However, the ideal condition of a steady flow hardly occurs in the real-time industry. Therefore, the unsteady flow becomes an important topic of study. The unsteady shrinking sheet problem with a mass suction has been studied for both Newtonian and non-Newtonian fluids, for example, Fang et al. [18] solved for the viscous fluid problem; Merkin and Kumaran [19] considered the MHD flow; Ali et al. [20] solved for the rotating fluid problem; Abbas et al. [21] studied the viscous fluid with partial slip condition; while Rohni et al. [22] and Bachok et al. [23] solved for the nanofluid problem. On the other hand, the unsteady boundary layer flow of micropolar fluids have been also investigated by several authors. El-Aziz [24] studied the unsteady mixed convection flow over a stretching surface in strong concentration micropolar fluid with viscous dissipation. The unsteady mixed convection of a magneto-micropolar fluid towards a permeable stretching or shrinking sheet with viscous dissipation has been studied by Sandeep and Sulochana [25]. They analyzed the effects of non-uniform heat sink or source, mass transfer and chemical reaction on the weak concentration micropolar fluid. Mohanty et al. [26] dealt with the problem of an unsteady mixed convection flow of a strong concentration micropolar fluid towards a stretching sheet in a porous medium with viscous dissipation and uniformed magnetic field. Recently, Roy et al. [27] analyzed the problem of unsteady weak concentration micropolar hybrid nanofluid flow over a stretching or shrinking sheet. Their numerical results provide dual solutions in terms of the velocity ratio parameter. It has to be mentioned here that the existence of triple solutions had been found in the research study by Naganthran et al. [28] for the problem of Carreau thin film flow over permeable and time-dependent shrinking velocity under the influence of thermocapillarity and injection. They found that only one solution can be physically realizable but the other two solutions are not realizable.

Motivated from the above studies, the aim of this paper is to study the problem of unsteady boundary layer flow of strong concentration micropolar fluid with suction and time-dependent shrinking velocity theoretically. The mathematical model of the problem is provided and solved numerically using Matlab's bvp4c program. The effects of governing parameters such as micropolar material parameter, shrinking parameter and suction parameter on the skin friction coefficient, velocity profile and microrotation profile are investigated. Since more than one solution is obtained for such a problem, hence stability analysis is performed to determine which solution branch is stable and physically realizable. The detail of the stability analysis for the stretching/shrinking problem can be found in the papers, see for example, by Hafidzuddin et al. [29], Awaludin et al. [30], Lok et al. [31] and Lund et al. [32].

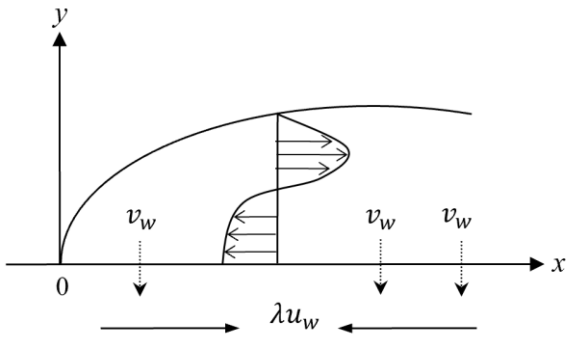

Figure 1. Physical model and coordinate system

PROBLEM FORMULATION

Figure 1 shows the flow configuration of a two-dimensional boundary layer flow over an unsteady permeable shrinking sheet in a micropolar fluid. The velocity of the sheet is time-dependent, $U_w(x,t) = ax/(1-\alpha t)$ where a is a positive constant with unit s^{-1} which represents the strength of linear velocity and t is the time, $t \neq 1/\alpha$. Following [18], α is defined as a constant with unit s^{-1} which showing the unsteadiness of the problem. The velocity of the sheet U_w is positive when $\alpha < 1/t$ while U_w is negative when $\alpha > 1/t$. The velocity of the mass suction $v_w(x,t)$ will be determined after the similarity transformation is performed. The Cartesian coordinates is defined by the x-axis which is measured along the plate, and the y-axis which is measured normal to the plate. Under these conditions, the unsteady two-dimensional boundary layer equations are [18, 25]

$$\frac{\partial u}{\partial x} + \frac{\partial v}{\partial y} = 0, \tag{1}$$

$$\frac{\partial u}{\partial t} + u\frac{\partial u}{\partial x} + v\frac{\partial u}{\partial y} = \left(\frac{\mu + \kappa}{\rho}\right)\frac{\partial^2 u}{\partial y^2} + \frac{\kappa}{\rho}\frac{\partial N}{\partial y}, \tag{2}$$

$$\rho j\left(\frac{\partial N}{\partial t}+u\frac{\partial N}{\partial x}+v\frac{\partial N}{\partial y}\right)=\gamma\frac{\partial^2 N}{\partial y^2}-\kappa\left(2N+\frac{\partial u}{\partial y}\right), \tag{3}$$

subject to the initial and boundary conditions

$$\begin{aligned} u=\lambda U_w(x,t), \quad v=v_w(x,t), \quad N=-n\frac{\partial u}{\partial y} \quad \text{at} \quad t\geq 0, \quad y=0, \\ u\to 0, \quad N\to 0 \quad \text{as} \quad y\to\infty, \end{aligned} \tag{4}$$

where u and v are the velocity components, N is microrotation vector normal to $x-y$ plane, μ is the dynamic viscosity, κ is the vortex viscosity, ρ is the fluid density, j is the microinertia density which is assumed to have the expression $j=\nu(1-\alpha t)/a$, ν is the kinematic viscosity, γ is the spin-gradient viscosity (a constant) which is given by $\gamma=(\mu+\kappa/2)j$ [9], $\lambda<0$ is the shrinking parameter and n is the ratio of the microrotation velocity component to the wall skin friction. Here, n can take values such that $0\leq n\leq 1$. The case $n=0$ refers to strong concentration of particles in micropolar fluids, $n=1/2$ indicates the weak concentration of micropolar fluid and $n=1$ is used for the modelling of turbulent boundary layer flow [7].

To obtain the similarity solutions, the following similarity variables are introduced

$$u=\frac{ax}{1-\alpha t}f'(\eta), v=-\sqrt{\frac{a\nu}{1-\alpha t}}f(\eta), N=\sqrt{\frac{a^3}{\nu(1-\alpha t)^3}}xg(\eta), \eta=\sqrt{\frac{a}{\nu(1-\alpha t)}}y \tag{5}$$

while the suction is defined as

$$v_w=-\sqrt{\frac{a\nu}{1-\alpha t}}s, \tag{6}$$

where $s>0$ is the mass suction parameter.

Substituting Eqs. (5) and (6) into Eqs. (1) to (4), the following ordinary differential equations are obtained

$$(1+K)f'''+ff''-f'^2-\beta\left(\frac{\eta}{2}f''+f'\right)+Kg'=0, \tag{7}$$

$$\left(1+\frac{K}{2}\right)g''-f'g+fg'-\beta\left(\frac{3}{2}g+\frac{\eta}{2}g'\right)-K(2g+f'')=0, \tag{8}$$

subject to the boundary conditions

$$\begin{aligned} f(0)=s, \quad f'(0)=\lambda, \quad g(0)=-nf''(0), \\ f'\to 0, \quad g\to 0, \quad \text{as} \quad \eta\to\infty, \end{aligned} \tag{9}$$

where $K=\mu/\kappa$ is the micropolar material parameter and $\beta=\alpha/a$ is the unsteadiness parameter. It is noticed that when $K=0$ (viscous fluid), Eq. (7) reduces to Eq. (6) in the paper by Fang et al. [18]. As mentioned by Fang et al. [18], Rohni et al. [22] and Roşca and Pop [33], the shrinking sheet is decelerating with $\beta\leq 0$.

The skin friction coefficient C_f and the wall shear stress τ_w are defined, respectively, as

$$C_f=\frac{\tau_w}{\rho U_w^2/2}, \quad \tau_w=\left[(\mu+\kappa)\frac{\partial u}{\partial y}+\kappa N\right]_{y=0} \tag{10}$$

Using Eqs. (5), (10) and boundary condition (9), the following skin friction coefficient is obtained

$$Re_x^{1/2}C_f=2[1+(1-n)K]f''(0) \tag{11}$$

where $Re_x=U_w x/\nu$ is the local Reynolds number.

STABILITY ANALYSIS

From the literature reviews, most of the shrinking sheet problems produced dual solutions. The time-dependent shrinking velocity that is considered in the present study inevitably showed that multiple solutions exist for some values of parameters that are considered. Hence, it is essential to carry out the stability analysis so that we can identify which of these solutions are stable and which are not. The stability analysis performed here requires a new dimensionless time variable τ which is correlated to an initial value problem [29, 30, 32, 34]. Therefore, the new variables that are similar to Eq. (5) but including the term τ for the problem (1)-(4) are

$$u = \frac{ax}{1-\alpha t}\frac{\partial f(\eta,\tau)}{\partial \eta}, \qquad v = -\sqrt{\frac{ax}{1-\alpha t}}f(\eta,\tau), \qquad N = \sqrt{\frac{a^3}{\nu(1-\alpha t)^3}}xg(\eta,\tau),$$
$$\eta = \sqrt{\frac{a}{\nu(1-\alpha t)}}y, \qquad \tau = at, \tag{12}$$

so that Eqs. (2) and (3) can be written as

$$(1+K)\frac{\partial^3 f}{\partial \eta^3} + f\frac{\partial^2 f}{\partial \eta^2} - \left(\frac{\partial f}{\partial \eta}\right)^2 - \beta\left(\frac{\eta}{2}\frac{\partial^2 f}{\partial \eta^2} + \frac{\partial f}{\partial \eta}\right) + K\frac{\partial g}{\partial \eta} - (1-\beta\tau)\frac{\partial^2 f}{\partial \tau \partial \eta} = 0, \tag{13}$$

$$\left(1+\frac{K}{2}\right)\frac{\partial^2 g}{\partial \eta^2} + f\frac{\partial g}{\partial \eta} - g\frac{\partial f}{\partial \eta} - \frac{\beta}{2}\left(3g + \eta\frac{\partial g}{\partial \eta}\right) - K\left(2g + \frac{\partial^2 f}{\partial \eta^2}\right) - (1-\beta\tau)\frac{\partial g}{\partial \tau} = 0, \tag{14}$$

with the boundary conditions

$$f(0,\tau) = s, \qquad \frac{\partial f}{\partial \eta}(0,\tau) = \lambda, \qquad g(0,\tau) = -n\frac{\partial^2 f}{\partial \eta^2}(0,\tau),$$
$$\frac{\partial f}{\partial \eta}(\eta,\tau) \to 0, \qquad g(\eta,\tau) \to 0 \quad \text{as} \quad \eta \to \infty \tag{15}$$

Following Merkin [35], let

$$f(\eta,\tau) = f_0(\eta) + e^{-\chi\tau}F(\eta,\tau), \qquad g(\eta,\tau) = g_0(\eta) + e^{-\chi\tau}G(\eta,\tau), \tag{16}$$

where $f(\eta) = f_0(\eta)$ and $g(\eta) = g_0(\eta)$ correspond to the similarity solution which satisfies Eqs. (7)-(9) while $F(\eta,\tau)$ and $G(\eta,\tau)$ are relatively small compared to $f_0(\eta)$ and $g_0(\eta)$, respectively. The exponential terms in Eq. (16) are treated as disturbance and the unknown parameter χ is defined as the eigenvalue parameter.

Substituting Eq. (16) into Eqs. (13) and (14), we obtain

$$(1+K)\frac{\partial^3 F}{\partial \eta^3} + f_0\frac{\partial^2 F}{\partial \eta^2} + [\chi(1-\beta\tau) - 2f_0']\frac{\partial F}{\partial x} + f_0''F - \beta\left(\frac{\eta}{2}\frac{\partial^2 F}{\partial \eta^2} + \frac{\partial F}{\partial \eta}\right)$$
$$+K\frac{\partial G}{\partial \eta} - (1-\beta\tau)\frac{\partial^2 F}{\partial \tau \partial \eta} = 0, \tag{17}$$

$$\left(1+\frac{K}{2}\right)\frac{\partial^2 G}{\partial \eta^2} + f_0'\frac{\partial G}{\partial \eta} + [\chi(1-\beta\tau) - f_0']G - g_0\frac{\partial F}{\partial \eta} + Fg_0' - \frac{\beta}{2}\left(3G + \eta\frac{\partial G}{\partial \eta}\right)$$
$$-K\left(2G + \frac{\partial^2 F}{\partial \eta^2}\right) - (1-\beta\tau)\frac{\partial G}{\partial \tau} = 0, \tag{18}$$

and the boundary conditions (15) now become

$$F(0,\tau) = 0, \qquad \frac{\partial F}{\partial \eta}(0,\tau) = 0, \qquad G(0,\tau) = -n\frac{\partial^2 F}{\partial \eta^2}(0,\tau),$$
$$\frac{\partial F}{\partial \eta}(\eta,\tau) \to 0, \qquad G(\eta,\tau) \to 0, \quad \text{as} \quad \eta \to \infty. \tag{19}$$

The stability of the flow solution $f_0(\eta)$ and $g_0(\eta)$ is investigated by setting $\tau = 0$ where $F(\eta) = F_0(\eta)$ and $G(\eta) = G_0(\eta)$ in Eqs. (17)-(19) indicate the initial growth or decay of the solution (16) [34, 35]. Hence, we obtain the following linearized equations

$$(1+K)F_0''' + f_0F_0'' + f_0''F_0 + (\chi - 2f_0')F_0' - \beta\left(\frac{\eta}{2}F_0'' + F_0'\right) + KG_0' = 0 \tag{20}$$

$$\left(1+\frac{K}{2}\right)G_0'' + f_0'G_0' - g_0F_0' + F_0g_0' + (\chi - f_0')G_0 - \frac{\beta}{2}(3G_0 + \eta G_0') - K(2G_0 + F_0'') = 0, \tag{21}$$

along with the boundary conditions

$$F_0(0) = 0, \quad F_0'(0) = 0, \quad G_0(0) = -nF_0''(0), \\ F_0'(\eta) \to 0, \quad G_0(\eta) \to 0, \quad \text{as} \quad \eta \to \infty. \tag{22}$$

Using the numerical values of $f(\eta) = f_0(\eta)$ and $g(\eta) = g_0(\eta)$ that obtained from solving the Eqs. (7)-(9), we can solve Eqs. (20)-(22) numerically. The stability of the solution $f_0(\eta)$ and $g_0(\eta)$ can be identified by examining the value of the smallest eigenvalue χ_1. Here, χ_1 can take a positive or negative value. If χ_1 is positive and $\tau \to \infty$, the solution (16) goes to $f_0(\eta)$ and $g_0(\eta)$, which are also the solutions of Eqs. (7)-(9), therefore there is an initial decay of disturbance and the solution is stable and physically realizable. If χ_1 is negative, there is an initial growth of disturbance, hence the solution is unstable. From Harris et al. [36], the values of eigenvalues can be found by relaxing a boundary condition at the infinity (far-field condition). In this paper, we relax the boundary condition $G_0(\eta) \to 0$ as $\eta \to \infty$, so that boundary conditions (22) now become:

$$F_0(0) = 0, \quad F_0'(0) = 0, \quad G_0(0) = -nF_0''(0), \quad G_0'(0) = 1, \\ F_0'(\eta) \to 0, \quad \text{as} \quad \eta \to \infty \tag{23}$$

NUMERICAL METHOD

The numerical solutions of the ordinary differential Eqs. (7) and (8) together with the boundary conditions (9) have been obtained using the *bvp4c* program in Matlab®. In this study, the relative error of tolerance is set to 10^{-7}. The boundary layer thickness η is represented as 'infinity' in the boundary condition (9). Here, the values of the boundary layer thickness range from $\eta = 20$ to $\eta = 35$. It is found that using the same initial guesses but different values of η will give us non-unique solutions. However, in some cases, with the same boundary layer thickness but different initial guesses, different solutions will be obtained. The continuation tactic is used to overcome the cases when it is difficult to provide suitable initial guesses for the solution. Shampine et al. [37] gave examples and tutorials of solving the boundary value problem using the *bvp4c*. Validation of the bvp4c method and program has been done by comparing the suction's critical values with those of Bhattacharyya et al. [14] when $\beta = 0$ (steady flow) and $\lambda = -1$ (shrinking case) for different values of micropolar material parameters. The comparison is shown in Table 1.

Table 1. Comparison of critical values of suction, s_c for steady flow ($\beta = 0$) and shrinking case ($\lambda = -1$)

n	K	s_c	
		Battacharyya et al. [14]	Present result
0	0.1	2.09041	2.09058
0.5	0.1	2.04895	2.04922
	0.2	2.09682	2.09732
1	0.1	2.00258	2.00314

In addition, we have compared in Figure 2 the results for $f''(0)$ against unsteadiness parameter β, with those by Fang et al. [18] for a viscous fluid ($K = 0$), $\lambda = -1$ (shrinking sheet) and several values of suction parameter s. We found a favorable agreement with the results obtained by Fang et al. [18].

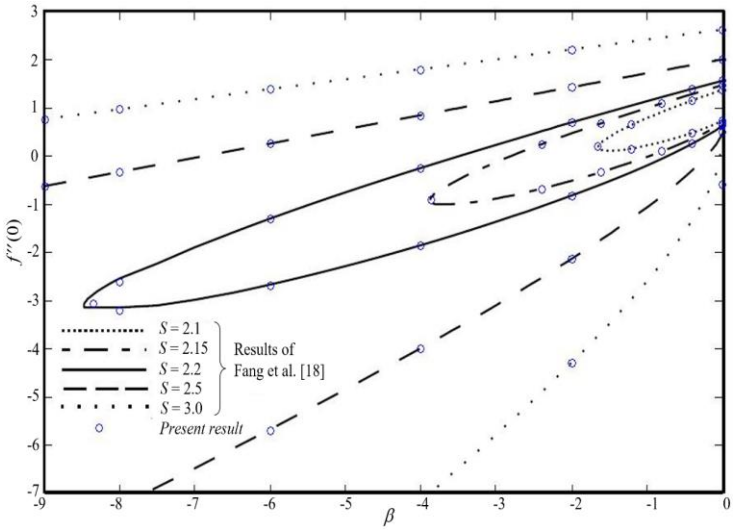

Figure 2. Comparison of $f''(0)$ with those by Fang et al. [18] for $K = 0, \lambda = -1$ and several values of s and β

RESULTS AND DISCUSSION

Numerical results are presented graphically for some values of the micropolar material parameter K, the unsteadiness parameter β, the shrinking parameter λ and the mass suction parameter s on the skin friction coefficient $Re_x^{1/2}C_f$, the initial values $g'(0)$, velocity profiles $f'(\eta)$ and microrotation profiles $g(\eta)$. Here we consider only the case of strong concentration $(n = 0)$ micropolar fluid. It is found that by solving this model mathematically, more than one solution is obtained. This phenomenon is common when solving a boundary value problem. In contrast to the initial value problem that usually has a unique solution, there are three possibilities of the type of solutions for a boundary value problem, i.e. no solution; a unique solution; or more than one solution (maybe a finite or infinite number of solutions) [37]. We observed from Figures 3 and 4 that the systems of Eqs. (7)-(9) for micropolar fluid $(K > 0)$ gave multiple (triple) solutions, compared to only dual solutions for the viscous fluid $(K = 0)$. Hence, the existence of an extra solution is due to the effect of microrotation of the particles in a micropolar fluid. The solutions in Figures 3 and 4 are labelled in such a way that the linear line is named as the first branch solution, while the second and the third solution form the bifurcation where the critical values λ_c are identified and stated in Figures 3 and 4. It can be seen from Figure 3 that the first branch solution decreases linearly to the decrement of λ while in Figure 4, the first branch solution increases monotonically as λ increases.

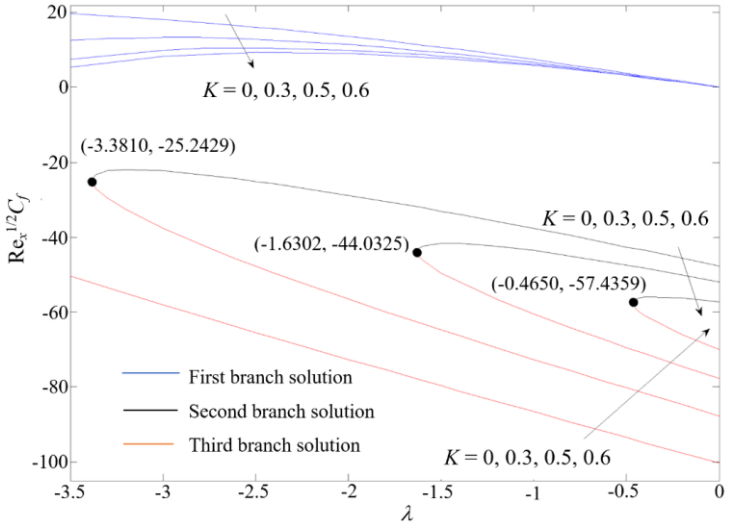

Figure 3. Plot of $Re_x^{1/2}C_f$ against λ for various values of K when $s = 5, \beta = -10$ and $n = 0$

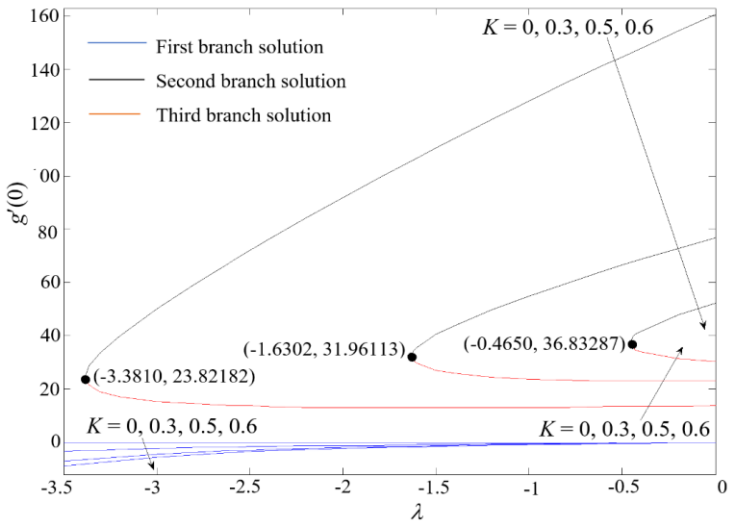

Figure 4. The plot of $g'(0)$ against λ for various values of K when $s = 5, \beta = -10$ and $n = 0$

In order to determine the stability of the triple solutions, we looked for the values of eigenvalues χ in Eq. (16) by numerically solving Eqs. (20) and (21) subject to the boundary conditions (23) using the *bvp4c* program. The smallest eigenvalues χ_1 for some values of K and λ when $\beta = -10, s = 5$ and $n = 0$ are presented in Table 2. It is obvious from Table 2 that the first and the second branch of the solutions have positive eigenvalues. Based on the stability analysis, we can conclude that the first and the second branch of the solutions are physically realizable due to an initial decay of disturbance when $\chi_1 > 0$ and $\tau \to \infty$, therefore is denoted as stable. The third branch solution has a negative value of χ_1

which corresponds to an initial growth of disturbances, therefore it is physically unrealizable hence is denoted as unstable. The results of the stability analysis explained the same profile trends that are observed for both the first and the second branch solutions (stable solution) where the skin friction coefficient decreases as K increases, while the opposite trend is observed for the third solution which is categorized as an unstable solution. On the other hand, we notice from Table 2 that as the value of λ approaches the critical value λ_c when $K > 0$, the smallest eigenvalue for the second branch solution (positive value) and the third branch solution (negative value) become smaller and approaching zero. Since the third branch solution is physically unrealizable, the discussion of the result focuses more on the first and the second branch solutions.

Figures 5-8 plot the triple solutions of velocity profiles and microrotation profiles for the effects of K, β, λ and s. From these figures, it is obvious that for all $f'(\eta)$ and $g(\eta)$, the boundary layer thickness for the first branch solutions is smaller than that for the second and the third branch solutions. Furthermore, it can be seen from these figures that all three branches of solutions asymptotically satisfied the boundary conditions (9) at infinity. This supports the validity of the existence of the triple solutions, at least mathematically, that are shown in Figures 3 and 4. Generally, the velocity profiles of the first branch solution increase gradually as η increases (far from the boundary surface). However, the velocity profiles of the second branch solution and the third branch solution start with a negative velocity gradient and are then distributed in a parabolic trajectory. To investigate the effect of K, we set the fixed values of $\beta = -12, \lambda = -1$ and $s = 5$. It is observed from Figure 5(a) that the momentum boundary layer thickness of triple solutions increases with K. This is due to the fact that an increase in the micropolar material parameter enhances the velocity. The plots of the velocity and microrotation profiles with η for some values of β are presented in Figure 6. The second branch solution for $f'(\eta)$ and $g(\eta)$ show larger boundary layer thickness when compared to the first branch solution as illustrated in Figures 6(a) and 6(b). The enhancement of the unsteadiness parameter increases the velocity profile. This agrees with the findings of Gupta et al. [38]. As discussed by Fang et al. [18], a higher magnitude of β make the fluid velocity damped faster, this can be seen from the shorter penetration of velocity into the fluid in Figure 6(a).

Table 2. The smallest eigenvalues χ_1 at several values of λ for some values of K when $\beta = -10, s = 5$ and $n = 0$

K	λ	χ_1		
		First branch	Second branch	Third branch
0	0	9.1100	-	-5.0000
	-0.50	8.6780	-	-4.8557
	-1.00	8.2100	-	-4.6942
0.3	-2.00	6.6623	2.7734	-2.6726
	-3.00	5.4829	1.5330	-1.5089
	-3.36	4.5832	0.3682	-0.3671
	-3.38	4.5299	0.0835	-0.0834
0.5	-1.00	7.8800	1.6129	-1.5811
	-1.50	7.0885	0.7546	-0.7479
	-1.60	6.9131	0.3655	-0.3639
	-1.62	6.8776	0.2130	-0.2124
0.6	-0.20	8.5930	0.9101	-0.8998
	-0.40	8.3008	0.4532	-0.4507
	-0.43	8.2562	0.3309	-0.3295

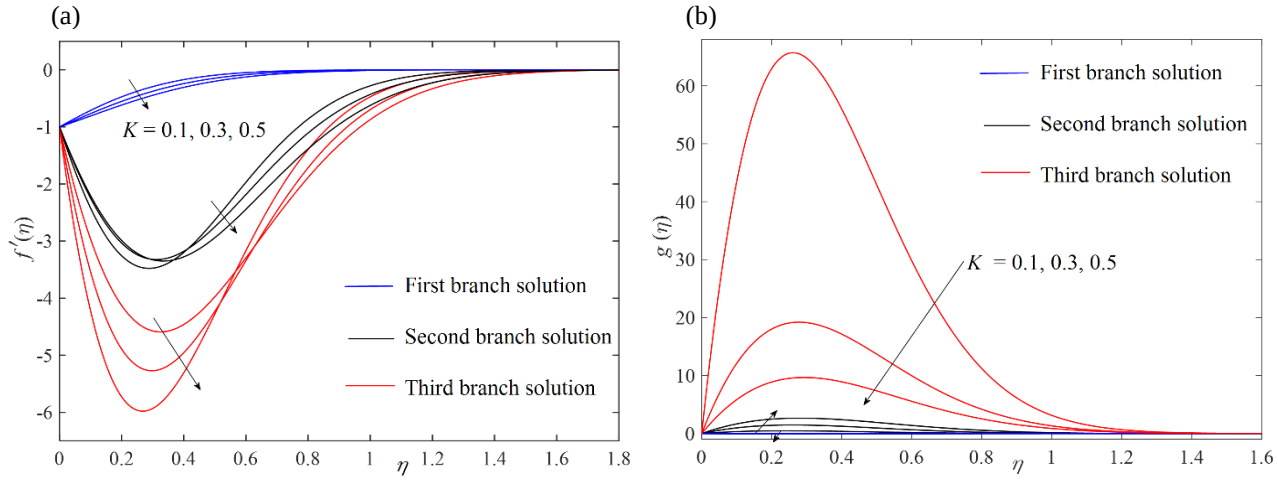

Figure 5. Effects of micropolar material parameter K with $\beta = -12, \lambda = -1$ and $s = 5$ for: (a) velocity profiles and (b) microrotation profiles

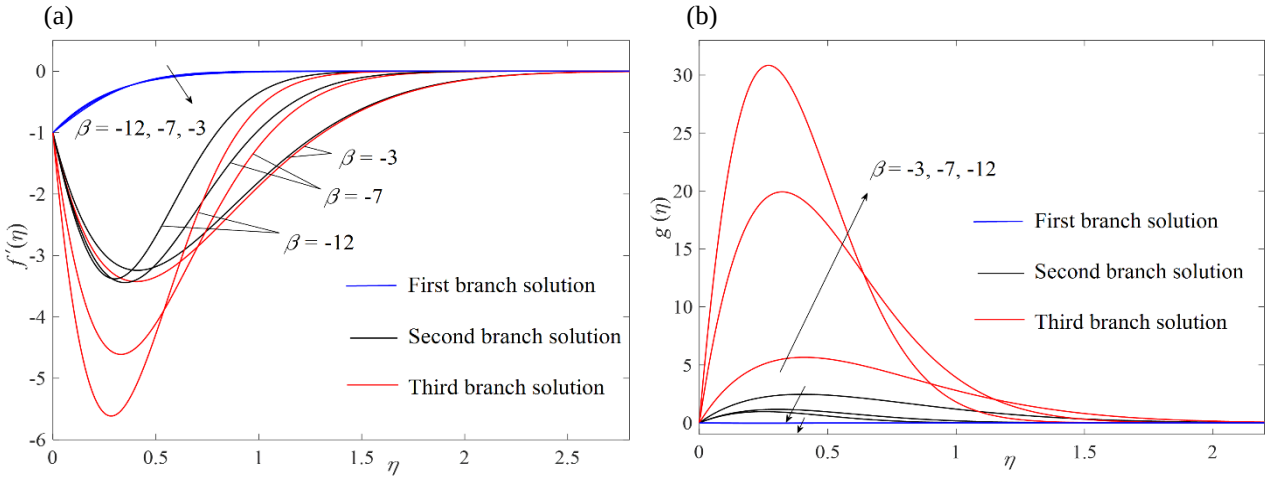

Figure 6. Effects of unsteadiness parameter β with $K = 0.2, \lambda = -1$ and $s = 5$ for: (a) velocity profiles and (b) microrotation profiles

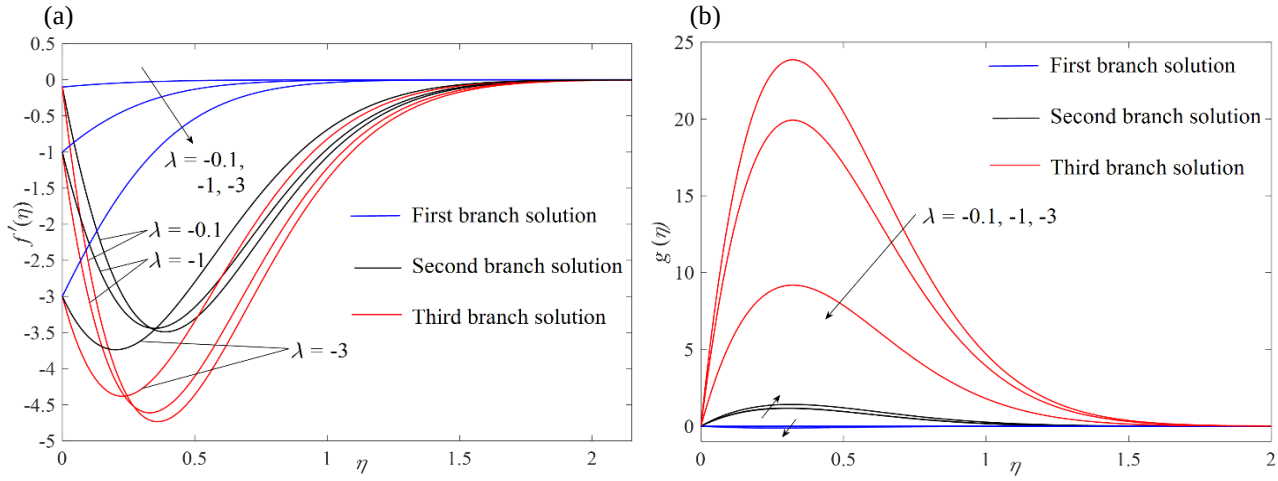

Figure 7. Effects of shrinking parameter λ with $K = 0.2, \beta = -7$ and $s = 5$ for: (a) velocity profiles and (b) microrotation profiles

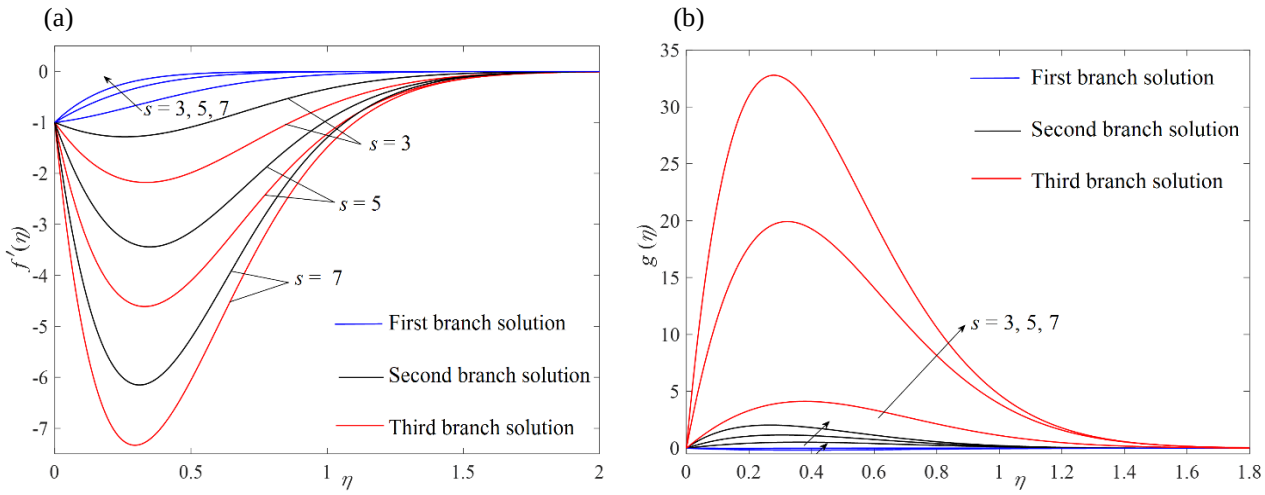

Figure 8. Effects of suction parameter s with $K = 0.2, \beta = -7$ and $\lambda = -1$ for: (a) velocity profiles and (b) microrotation profiles

To examine the effect of the shrinking parameter, the values of other parameters are fixed to $K = 0.2$, $\beta = -7$ and $s = 5$. The profiles for $f'(\eta)$ and $g(\eta)$ are shown in Figures 7(a) and 7(b) respectively for $\lambda = -0.1, -1, -3$. It is found that the velocity profiles of the triple solutions fall when λ increases. However, the microrotation for the first branch solution decreases while the second branch solution increases as λ increases. It shows in general, the effect of shrinking cause the reduction of fluid's microrotation, however, it enhanced the microrotation of fluid for the reversed flow (second branch solution). It is also found that boundary layer thickness increases by increasing the values of the shrinking parameter. Figure 8 illustrates the profiles of $f'(\eta)$ and $g(\eta)$ with η for different values of s. As studied by Miklavčič and Wang [11], and Fang and Zhang [39], shrinking sheet flow only occurs when the suction parameter is sufficiently large. As can be seen from Figure 8(a), the fluid velocity of the first branch solution is found to increase with the increase in the value of s. It is because the suction will increase the skin friction coefficient. For the second and the third branch solutions, reversed flow (negative value of velocity) is more profound for larger suction parameter. From Figure 8, it is found that the boundary layer thickness of the first branch solution decreases as s increases. Also, for the first branch solution, the penetration of the velocity into the fluid is short when the value of suction parameter increases. From the observation of the second and the third branch solutions, the velocity penetration becomes deeper with the increase of the suction parameter. These observations are in accordance with those reported by Fang et al. [18]. The microrotation profile of the triple solutions is observed to increase as s increases.

CONCLUSIONS

The problem of the unsteady boundary layer flow of a time-dependent shrinking sheet velocity with suction in a strong concentration of micropolar fluid has been studied. The governing partial differential equations are succeeded to reduce to ODEs by introducing the similarity variables. The problem has been numerically solved using the boundary value problem solver in Matlab®, i.e. the *bvp4c* program. Numerical solutions for the skin friction coefficient $Re_x^{1/2} C_f$, the initial values $g'(0)$, velocity profiles $f'(\eta)$ and microrotation profiles $g(\eta)$ are graphically presented. The following findings are obtained:

- By solving the model numerically, triple solutions are found.
- The performed stability analysis showed that there are two branches of solutions that are linearly stable. Hence, these two solutions are treated as physically meaningful solutions. There exists the third branch solution which is linearly unstable and physically not realizable.
- For a fixed suction parameter and unsteadiness parameter, the skin friction coefficient of the first and the second branch solutions decreases with the increase of micropolar material and shrinking parameters.
- Boundary layer thickness for the second branch solution is greater than that for the first branch solution.
- The velocity profile for the first branch solution increases as the flow is away from the boundary surface while the second branch solutions show the existence of reversed flow (negative value of f').
- Based on the results from the first branch solutions, the velocity of the flow increases as the unsteadiness parameter and suction parameter are increasing. An opposite trend is observed for the case of micropolar material parameter and shrinking parameter.
- For the microrotation of the flow, it decreases as the micropolar material parameter, unsteadiness parameter and shrinking parameter are increasing. The suction parameter caused the reverse trend.

ACKNOWLEDGMENTS

The authors would like to acknowledge the financial support received from the Ministry of Higher Education, Malaysia under the Fundamental Research Grant Scheme (FRGS), project code: FRGS/1/2018/STG06/USM/02/5.

REFERENCES

[1] A. C. Eringen, "Theory of micropolar fluids," *J. Math. Mech.*, vol. 16, no. 1, pp. 1–18, 1966.

[2] G. Łukaszewicz, *Micropolar Fluids: Theory and Applications*. Boston, U.S.: Birkhäuser, 1999.

[3] A. C. Eringen, *Microcontinuum Field Theories: I. Foundations and Solids*. New York, U.S.: Springer-Verlag, 1999.

[4] T. Ariman, M. A. Turk, and N. D. Sylvester, "Microcontinuum fluid mechanics—A review," *Int. J. Eng. Sci.*, vol. 11, no. 8, pp. 905–930, 1973, doi: https://doi.org/10.1016/0020-7225(73)90038-4.

[5] T. Ariman, M. A. Turk, and N. D. Sylvester, "Applications of microcontinuum fluid mechanics," *Int. J. Eng. Sci.*, vol. 12, no. 4, pp. 273–293, 1974, doi: https://doi.org/10.1016/0020-7225(74)90059-7.

[6] A. J. Willson, "Boundary layers in micropolar liquids," *Math. Proc. Cambridge Philos. Soc.*, vol. 67, no. 2, pp. 469–476, 1970, doi: DOI: 10.1017/S0305004100045746.

[7] J. Peddieson, "Boundary layer theory for a micropolar fluid," Virginia Polytechnic Institute and State University, U.S., 1969.

[8] R. S. R. Gorla, "Combined forced and free convection in micropolar boundary layer flow on a vertical flat plate," *Int. J. Eng. Sci.*, vol. 26, no. 4, pp. 385–391, 1988, doi: https://doi.org/10.1016/0020-7225(88)90117-6.

[9] D. A. S. Rees and A. P. Bassom, "The Blasius boundary-layer flow of a micropolar fluid," *Int. J. Eng. Sci.*, vol. 34, no. 1, pp. 113–124, 1996, doi: https://doi.org/10.1016/0020-7225(95)00058-5.

[10] E. G. Fisher, E. C. Whitfield, and Plastics and Rubber Institute, *Extrusion of Plastics*, 3rd ed. New York, U.S.: Halsted Press, 1976.

[11] M. Miklavčič and C. Y. Wang, "Viscous flow due to a shrinking sheet," *Quart. Appl. Math.*, vol. 64, no. 2, pp. 283–290, 2006, doi: 10.1090/S0033-569X-06-01002-5.

[12] S. Goldstein, "On backward boundary layers and flow in converging passages," *J. Fluid Mech.*, vol. 21, no. 1, pp. 33–45, 1965, doi: DOI: 10.1017/S0022112065000034.

[13] N. A. Yacob and A. Ishak, "Micropolar fluid flow over a shrinking sheet," *Meccanica*, vol. 47, no. 2, pp. 293–299, 2012, doi: 10.1007/s11012-011-9439-8.

[14] K. Bhattacharyya, S. Mukhopadhyay, G. C. Layek, and I. Pop, "Effects of thermal radiation on micropolar fluid flow and heat transfer over a porous shrinking sheet," *Int. J. Heat Mass Transf.*, vol. 55, no. 11, pp. 2945–2952, 2012, doi: https://doi.org/10.1016/j.ijheatmasstransfer.2012.01.051.

[15] H. Rosali, A. Ishak, and I. Pop, "Micropolar fluid flow towards a stretching/shrinking sheet in a porous medium with suction," *Int. Commun. Heat Mass Transf.*, vol. 39, no. 6, pp. 826–829, 2012, doi: https://doi.org/10.1016/j.icheatmasstransfer.2012.04.008.

[16] M. Turkyilmazoglu, "A note on micropolar fluid flow and heat transfer over a porous shrinking sheet," *Int. J. Heat Mass Transf.*, vol. 72, pp. 388–391, 2014, doi: https://doi.org/10.1016/j.ijheatmasstransfer.2014.01.039.

[17] N. C. Roşca and I. Pop, "Boundary layer flow past a permeable shrinking sheet in a micropolar fluid with a second-order slip flow model," *Eur. J. Mech. - B/Fluids*, vol. 48, pp. 115–122, 2014, doi: https://doi.org/10.1016/j.euromechflu.2014.05.004.

[18] T. G. Fang, J. Zhang, and S. S. Yao, "Viscous flow over an unsteady shrinking sheet with mass transfer," *Chinese Phys. Lett.*, vol. 26, no. 1, p. 14703, 2009, doi: 10.1088/0256-307X/26/1/014703.

[19] J. H. Merkin and V. Kumaran, "The unsteady MHD boundary-layer flow on a shrinking sheet," *Eur. J. Mech. - B/Fluids*, vol. 29, no. 5, pp. 357–363, 2010, doi: https://doi.org/10.1016/j.euromechflu.2010.03.006.

[20] F. M. Ali, R. Nazar, N. M. Arifin, and I. Pop, "Unsteady shrinking sheet with mass transfer in a rotating fluid," *Int. J. Numer. Methods Fluids*, vol. 66, no. 11, pp. 1465–1474, Aug. 2011, doi: 10.1002/fld.2325.

[21] Z. Abbas, S. Rasool, and M. M. Rashidi, "Heat transfer analysis due to an unsteady stretching/shrinking cylinder with partial slip condition and suction," *Ain Shams Eng. J.*, vol. 6, no. 3, pp. 939–945, 2015, doi: https://doi.org/10.1016/j.asej.2015.01.004.

[22] A. M. Rohni, S. Ahmad, and I. Pop, "Flow and heat transfer over an unsteady shrinking sheet with suction in nanofluids," *Int. J. Heat Mass Transf.*, vol. 55, no. 7, pp. 1888–1895, 2012, doi: https://doi.org/10.1016/j.ijheatmasstransfer.2011.11.042.

[23] N. Bachok, A. Ishak, and I. Pop, "Unsteady boundary-layer flow and heat transfer of a nanofluid over a permeable stretching/shrinking sheet," *Int. J. Heat Mass Transf.*, vol. 55, no. 7, pp. 2102–2109, 2012, doi: https://doi.org/10.1016/j.ijheatmasstransfer.2011.12.013.

[24] M. Abd El-Aziz, "Mixed convection flow of a micropolar fluid from an unsteady stretching surface with viscous dissipation," *J. Egypt. Math. Soc.*, vol. 21, no. 3, pp. 385–394, 2013, doi: https://doi.org/10.1016/j.joems.2013.02.010.

[25] N. Sandeep and C. Sulochana, "Dual solutions for unsteady mixed convection flow of MHD micropolar fluid over a stretching/shrinking sheet with non-uniform heat source/sink," *Eng. Sci. Technol. an Int. J.*, vol. 18, no. 4, pp. 738–745, 2015, doi: https://doi.org/10.1016/j.jestch.2015.05.006.

[26] B. Mohanty, S. R. Mishra, and H. B. Pattanayak, "Numerical investigation on heat and mass transfer effect of micropolar fluid over a stretching sheet through porous media," *Alexandria Eng. J.*, vol. 54, no. 2, pp. 223–232, 2015, doi: https://doi.org/10.1016/j.aej.2015.03.010.

[27] N. C. Roy, M. A. Hossain, and I. Pop, "Analysis of dual solutions of unsteady micropolar hybrid nanofluid flow over a stretching/shrinking sheet", *J. Appl. Comput. Mech.*, vol. 7, no. 1, pp. 19–33, 2021, doi: 10.22055/jacm.2020.34686.2457.

[28] K. Naganthran, I. Hashim, and R. Nazar, "Triple solutions of Carreau thin film flow with thermocapillarity and injection on an unsteady stretching sheet," *Energies*, vol. 13, no. 12. 2020, doi: 10.3390/en13123177.

[29] E. H. Hafidzuddin, R. Nazar, N. M. Arifin, and I. Pop, "Stability analysis of unsteady three-dimensional viscous flow over a permeable stretching/shrinking surface," *J. Qual. Meas. Anal.*, vol. 11, no. 1, pp. 19–31, 2015.

[30] I. S. Awaludin, P. D. Weidman, and A. Ishak, "Stability analysis of stagnation-point flow over a stretching/shrinking sheet," *AIP Adv.*, vol. 6, no. 4, p. 45308, 2016, doi: 10.1063/1.4947130.

[31] Y. Y. Lok, A. Ishak, and I. Pop, "Oblique stagnation slip flow of a micropolar fluid towards a stretching/shrinking surface: A stability analysis," *Chinese J. Phys.*, vol. 56, no. 6, pp. 3062–3072, 2018, doi: https://doi.org/10.1016/j.cjph.2018.10.016.

[32] L. A. Lund, Z. Omar, U. Khan, I. Khan, D. Baleanu, and K. S. Nisar, "Stability analysis and dual solutions of micropolar nanofluid over the inclined stretching/shrinking surface with convective boundary condition," *Symmetry*, vol. 12, no. 1. 2020, doi: 10.3390/sym12010074.

[33] N. C. Roşca and I. Pop, "Unsteady boundary layer flow over a permeable curved stretching/shrinking surface," *Eur. J. Mech. - B/Fluids*, vol. 51, pp. 61–67, 2015, doi: https://doi.org/10.1016/j.euromechflu.2015.01.001.

[34] P. D. Weidman, D. G. Kubitschek, and A. M. J. Davis, "The effect of transpiration on self-similar boundary layer flow over moving surfaces," *Int. J. Eng. Sci.*, vol. 44, no. 11, pp. 730–737, 2006, doi: https://doi.org/10.1016/j.ijengsci.2006.04.005.

[35] J. H. Merkin, "On dual solutions occurring in mixed convection in a porous medium," *J. Eng. Math.*, vol. 20, no. 2, pp. 171–179, 1986, doi: 10.1007/BF00042775.

[36] S. D. Harris, D. B. Ingham, and I. Pop, "Mixed convection boundary-layer flow near the stagnation point on a vertical surface in a porous medium: Brinkman model with slip," *Transp. Porous Media*, vol. 77, no. 2, pp. 267–285, 2009, doi: 10.1007/s11242-008-9309-6.

[37] L. F. Shampine, I. Gladwell, and S. Thompson *Solving ODEs with MATLAB*. Cambridge, U.K.: Cambridge University Press, 2003.

[38] D. Gupta, L. Kumar, and B. Singh, "Finite element solution of unsteady mixed convection flow of micropolar fluid over a porous shrinking sheet," *Sci. World J.*, vol. 2014, p. 362351, 2014, doi: 10.1155/2014/362351.

[39] T. Fang and J. Zhang, "Closed-form exact solutions of MHD viscous flow over a shrinking sheet," *Commun. Nonlinear Sci. Numer. Simul.*, vol. 14, no. 7, pp. 2853–2857, 2009, doi: https://doi.org/10.1016/j.cnsns.2008.10.005.